

The fingerprint of the summer 2018 drought in Europe on ground-based atmospheric CO 2 measurements

Michel Ramonet, Philippe Ciais, Francesco Apadula, Jakub Bartyzel, Ana Bastos, Peter Bergamaschi, Pierre-Éric Blanc, Dominik Brunner, Luigi Caracciolo Di Torchiarolo, Francescopiero Calzolari, et al.

▶ **To cite this version:**

Michel Ramonet, Philippe Ciais, Francesco Apadula, Jakub Bartyzel, Ana Bastos, et al.. The fingerprint of the summer 2018 drought in Europe on ground-based atmospheric CO 2 measurements. Philosophical Transactions of the Royal Society B: Biological Sciences, 2020, 375 (1810), pp.20190513. 10.1098/rstb.2019.0513 . hal-02938994

HAL Id: hal-02938994
https://hal.science/hal-02938994

Submitted on 4 Nov 2020

HAL is a multi-disciplinary open access archive for the deposit and dissemination of scientific research documents, whether they are published or not. The documents may come from teaching and research institutions in France or abroad, or from public or private research centers.

L'archive ouverte pluridisciplinaire **HAL**, est destinée au dépôt et à la diffusion de documents scientifiques de niveau recherche, publiés ou non, émanant des établissements d'enseignement et de recherche français ou étrangers, des laboratoires publics ou privés.

The fingerprint of the summer 2018 drought in Europe on ground-based atmospheric CO_2 measurements

M. Ramonet[1], P. Ciais[1], F. Apadula[25], J. Bartyzel[33], A. Bastos[35], P. Bergamaschi[20], P. E. Blanc[15], D. Brunner[26], L. Caracciolo di Torchiarolo[18], F. Calzolari[17], H. Chen[4], L. Chmura[33], A. Colomb[28], S. Conil[7], P. Cristofanelli[17], E. Cuevas[19], R. Curcoll[14], M. Delmotte[1], A. di Sarra[34], L. Emmenegger[26], G. Forster[30], A. Frumau[23], C. Gerbig[22], F. Gheusi[21], S. Hammer[31], L. Haszpra[12], J. Hatakka[10], L. Hazan[1], M. Heliasz[3], S. Henne[26], A. Hensen[23], O. Hermansen[24], P. Keronen[16], R. Kivi[10], K. Komínková[5], D. Kubistin[6], O. Laurent[1], T. Laurila[10], J. V. Lavric[22], I. Lehner[3], K. E. J. Lehtinen[37,10], A. Leskinen[37,10], M. Leuenberger[29], I. Levin[31], M. Lindauer[6], M. Lopez[1], C. Lund Myhre[24], I. Mammarella[16], G. Manca[20], A. Manning[30], M. V. Marek[5], P. Marklund[11], D. Martin[9], F. Meinhardt[27], N. Mihalopoulos[8], M. Mölder[40], J. A. Morgui[14], J. Necki[33], S. O'Doherty[2], C. O'Dowd[32], M. Ottosson[11], C. Philippon[1], S. Piacentino[34], J. M. Pichon[28], C. Plass-Duelmer[6], A. Resovsky[1], L. Rivier[1], X. Rodó[38,39], M. K. Sha[41], H. A. Scheeren[4], D. Sferlazzo[34], T. G. Spain[32], K. M. Stanley[2,36], M. Steinbacher[26], P. Trisolino[17], A. Vermeulen[13], G. Vítková[5], D. Weyrauch[6], I. Xueref-Remy[15], K. Yala[1] and C. Yver Kwok[1]

[1]Université Paris-Saclay, CEA, CNRS, UVSQ, Laboratoire des Sciences du Climat et de l'Environnement (LSCE/IPSL), Gif-sur-Yvette, France
[2]Atmospheric Chemistry Research Group School of Chemistry, University of Bristol, Bristol, UK
[3]Centre for Environmental and Climate Research, Lund University, Lund, Sweden
[4]Centre for Isotope Research (CIO), University of Groningen, Nijenborgh 6, 9747 AG Groningen, The Netherlands
[5]Global Change Research Institute of the Czech Academy of Sciences, Brno, Czech Republic
[6]Deutscher Wetterdienst, Hohenpeißenberg Meteorological Observatory, Hohenpeißenberg, Germany
[7]DRD/OPE, Andra, Bure, France
[8]Environmental Chemical Processes Laboratory, University of Crete, Greece
[9]Environmental Protection Agency, Dublin, Ireland
[10]Finnish Meteorological Institute, Helsinki, Finland
[11]Swedish University of Agricultural Sciences, Unit for Field-based Forest Research, 92291 Vindeln, Sweden
[12]Research Centre for Astronomy and Earth Sciences, Sopron, Hungary
[13]ICOS-ERIC, Carbon Portal, Lund, Sweden
[14]Institut de Ciencia i Tecnologia Ambientals, Universitat Autonoma de Barcelona, Barcelona, Spain
[15]Aix Marseille Univ, Avignon Université, CNRS, IRD, Institut Méditerranéen de Biodiversité et d'Ecologie marine et continentale (IMBE), Marseille, France
[16]Institute for Atmospheric and Earth System Research (INAR), University of Helsinki, Helsinki, Finland
[17]National Research Council, Institute of Atmospheric Sciences and Climate, Bologna, Italy
[18]Italian Air Force Meteorological Service, Rome, Italy
[19]Izana Atmospheric Research Center, Meteorological State Agency of Spain, Tenerife, Spain
[20]European Commission, Joint Research Centre, Ispra, Italy
[21]Laboratoire d'Aérologie, UPS Université Toulouse 3, CNRS (UMR5560), Toulouse, France
[22]Max Planck Institute for Biogeochemistry, Jena, Germany
[23]Netherlands Organisation for Applied Scientific Research, Petten, The Netherlands
[24]NILU - Norwegian Institute for Air Research, Oslo, Norway
[25]Ricerca sul Sistema Energetico, Milan, Italy
[26]Empa, Swiss Federal Laboratories for Materials Science and Technology, Duebendorf, Switzerland
[27]Umweltbundesamt, Berlin, Germany
[28]Université Clermont Auvergne, CNRS, Laboratoire de Météorologie Physique, UMR 6016, Clermont-Ferrand, France

Research

http://dx.doi.org/10.1098/rstb.2019.0513

Accepted: 28 February 2020

Subject Areas:
environmental science

Keywords:
atmospheric CO_2 measurements, net ecosystem exchange, drought, ICOS

Author for correspondence:
M. Ramonet
e-mail: michel.ramonet@lsce.ipsl.fr

[29]University of Bern, Physics Institute, Climate and Environmental Physics Division and Oeschger Center for Climate Change Research, Bern, Switzerland
[30]National Centre for Atmospheric Science, University of East Anglia, Norwich, UK
[31]University of Heidelberg, Institut fuer Umweltphysik, Heidelberg, Germany
[32]National University of Ireland Galway, Galway, Ireland
[33]AGH University of Science and Technology, 30059 Krakow, Poland
[34]Agenzia Nazionale per le Nuove Tecnologie, l'Energia e lo Sviluppo Economico Sostenibile, Rome, Italy
[35]Department of Geography, Ludwig-Maximilians University, 80333 Munich, Germany
[36]Institute for Atmospheric and Environmental Sciences, Goethe University Frankfurt, Frankfurt am Main, Germany
[37]University of Eastern Finland, Kuopio, Finland
[38]Climate and Health Programme (CLIMA), Barcelona Institute for Global Health (ISGLOBAL), Barcelona, Spain
[39]Institució Catalana de Recerca i Estudis Avancats (ICREA), Barcelona, Spain
[40]Department of Physical Geography and Ecosystem Science (INES), Lund University, Lund, Sweden
[41]Royal Belgian Institute for Space Aeronomy (BIRA-IASB), Brussels, Belgium

MR, 0000-0003-1157-1186; LH, 0000-0002-7747-6475; JVL, 0000-0003-3610-9078; ML, 0000-0001-9274-8750; MKS, 0000-0003-1440-1529; KMS, 0000-0003-3388-0932; PT, 0000-0003-1786-5310; AV, 0000-0002-8158-8787

During the summer of 2018, a widespread drought developed over Northern and Central Europe. The increase in temperature and the reduction of soil moisture have influenced carbon dioxide (CO_2) exchange between the atmosphere and terrestrial ecosystems in various ways, such as a reduction of photosynthesis, changes in ecosystem respiration, or allowing more frequent fires. In this study, we characterize the resulting perturbation of the atmospheric CO_2 seasonal cycles. 2018 has a good coverage of European regions affected by drought, allowing the investigation of how ecosystem flux anomalies impacted spatial CO_2 gradients between stations. This density of stations is unprecedented compared to previous drought events in 2003 and 2015, particularly thanks to the deployment of the Integrated Carbon Observation System (ICOS) network of atmospheric greenhouse gas monitoring stations in recent years. Seasonal CO_2 cycles from 48 European stations were available for 2017 and 2018. Earlier data were retrieved for comparison from international databases or national networks. Here, we show that the usual summer minimum in CO_2 due to the surface carbon uptake was reduced by 1.4 ppm in 2018 for the 10 stations located in the area most affected by the temperature anomaly, mostly in Northern Europe. Notwithstanding, the CO_2 transition phases before and after July were slower in 2018 compared to 2017, suggesting an extension of the growing season, with either continued CO_2 uptake by photosynthesis and/or a reduction in respiration driven by the depletion of substrate for respiration inherited from the previous months due to the drought. For stations with sufficiently long time series, the CO_2 anomaly observed in 2018 was compared to previous European droughts in 2003 and 2015. Considering the areas most affected by the temperature anomalies, we found a higher CO_2 anomaly in 2003 (+3 ppm averaged over 4 sites), and a smaller anomaly in 2015 (+1 ppm averaged over 11 sites) compared to 2018.

This article is part of the theme issue 'Impacts of the 2018 severe drought and heatwave in Europe: from site to continental scale'.

1. Introduction

Continuous atmospheric carbon dioxide (CO_2) measurements from ground-based networks provide very precise monitoring of long-term trends, as well as interannual, seasonal and daytime variations. These measurements can be used to derive information on surface fluxes. Analysis of spatial and temporal gradients in atmospheric CO_2 concentration measurements allows the detection of anomalies or unexpected behavior, e.g. due to persistent meteorological conditions that are expected to impact CO_2 fluxes [1–4]. We develop this approach in the present study, using an unprecedented dataset in Europe, in order to analyse the impact of the 2018 drought on atmospheric CO_2 concentrations. For a more quantitative approach, capable of estimating the anomaly on biospheric fluxes, it is necessary to use the observations in combination with atmospheric inverse models. Such models are used to optimize fluxes to best fit the atmospheric observations given simulated transport, and in most cases, given a prior estimate of fluxes and their uncertainty [5–9]. Atmospheric inversion models are comprehensive systems that provide optimized fluxes and their error statistic to best represent observed atmospheric concentrations. Generally, they assign uncertainties to atmospheric observations that are much larger than the instrumental uncertainty, to account for transport model uncertainties [10,11]. This approach is developed in three publications of the special issue [12–15], using the atmospheric CO_2 dataset that we describe in this article.

Our first goal is to present the most complete up-to-date, unpublished dataset of CO_2 atmospheric concentration measurements across Europe. Data of the harmonized integrated carbon observation system (ICOS) have only become available in recent years and have been combined with records from the same stations that were in operation before the implementation of ICOS, and with records from additional non-ICOS stations from regional and national networks. In this study, we carefully selected only stations that ensure a traceability of their measurements to the international World Meteorological Organization (WMO) CO_2 mole fraction scale [16,17]. The total number of sites with continuous, harmonized data are 48 stations in 2018, and cover the period from 1971 to the end of 2018. The second objective is to analyse the observed CO_2 concentration anomaly across different sites during the growing season of 2018 compared with previous years, mainly 2017, to answer the following question: can a dense atmospheric measurement network be used to directly detect the space–time patterns of CO_2 flux anomalies during the widespread and intense 2018 spring and summer drought event that prevailed over Northern and Central Europe?

2. The measurement stations

All atmospheric measurement stations operating continuous CO_2 measurements in 2018 are shown in figure 1. A total of 48 stations covering Western, Southern and Central Europe, and Nordic countries (table 1) are included. This network has a mean density of about 12 stations per 10^6 km^2 in the area of the countries that have at least two stations. There is no coverage in Belarus, Russia, or any country in the Balkans. The distance between one station and its three closest neighbours ranges from 60 to 80 km for stations located in the Alps

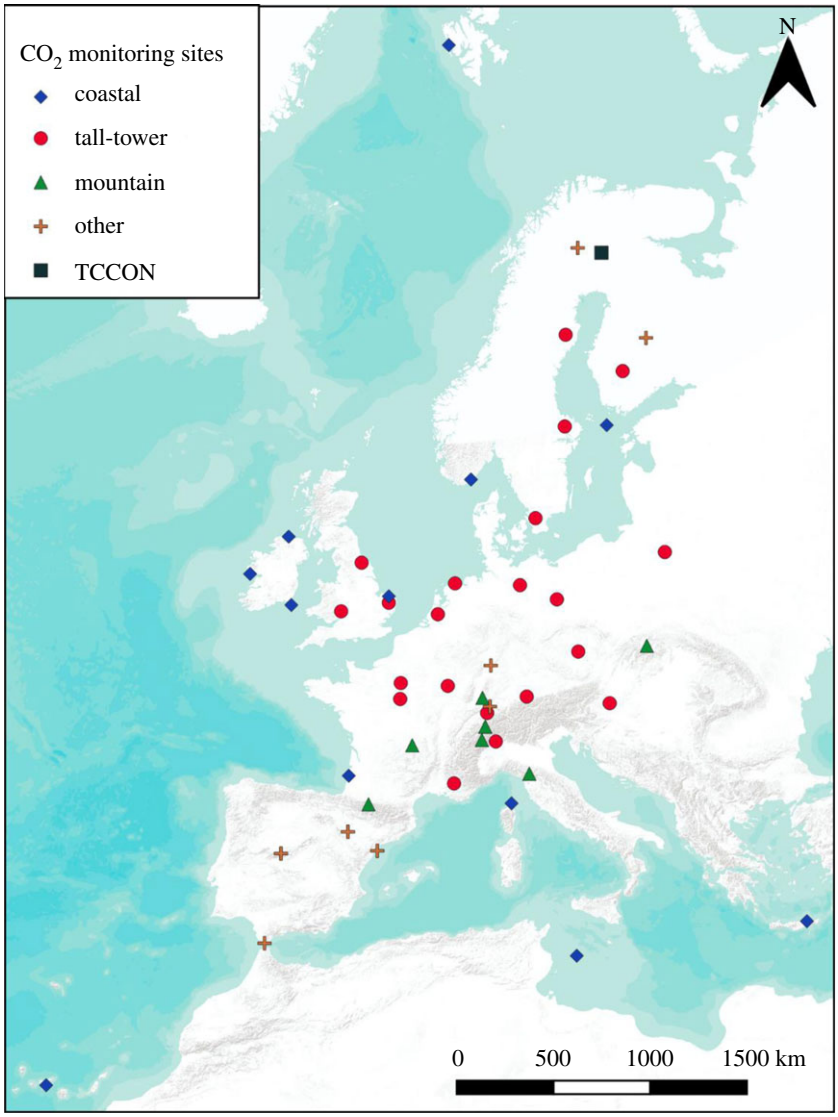


Figure 1. Location of the CO_2 monitoring sites in Europe. The symbols represent the different type of stations: tall towers (red circles), coastal sites (blue diamonds), mountain sites (green triangles), other surface stations (crosses) and total carbon column observing network (TCCON) site (square). (Online version in colour.)

(LHW, JFJ, BRM, PRS) to more than 1300 km for ZEP, FKL and IZO (table 1), and is equal to 385 km on average. The stations are located at tall towers in rural areas, mountain sites, coastal locations, and, in a few cases, in urban or suburban locations. Only 12 stations provided continuous data in 2009, in contrast to 48 in 2018. Tall tower measurements are generally made from two to five sampling levels ranging from 2.5 to 341 m above ground level. The present dataset contains 20 tall tower stations, which sums up to 68 time series corresponding to all sampling levels (table 1). In total, more than 5 million hourly averages of atmospheric CO_2 concentrations have been collected for this study. Depending on sites and time periods, data have been collected from different repositories (electronic supplementary material figure S1), namely: the National Oceanic and Atmospheric Administration's (NOAA) Observation Package (ObsPack) compilation (29%) [18], ICOS (26%), the World Data Centre for Greenhouse Gases (WDCGG) (5%), and from the scientists in charge of individual sites (40%). In this study, we use only *in situ* data, except for Lampedusa where concentrations from flasks sampled on a weekly basis [19] have been used in order to fill in a data gap from February to May 2018 at this station. The European research infrastructure ICOS is engaged in a process of standardization of measurement protocols, quality control and data processing for European stations [20,21]. The ICOS network represents a homogeneous subset of the European network (up to 55% of the total dataset in 2018), whose data are easily available through the ICOS Carbon Portal (www.icos-cp.eu), with high traceability, and it has been thoroughly evaluated by the ICOS scientific community. Data from the international repositories were checked for consistency prior to ingestion into the databases. Data from individual stations were validated by the responsible scientists. All measurements presented in this study are referenced to the international reference scale WMO-X2007 [17,22], and can be downloaded from the ICOS Carbon Portal (doi:10.18160/ere9–9d85).

Data availability and the temporal coverage of the data from 2008 to 2018 are represented in figure 2. The longest records are from Schauinsland, Germany (since 1971), and Monte Cimone, Italy (since 1979), and the shortest are from recently installed ICOS sites like Norunda (January 2017) and Svartberget (June 2017) in Sweden. New ICOS sites that have become operational since summer 2018 were not included in this analysis due to the measurement period being too short. Based on daily averages, rates of missing data during the measurement period can be classified in three tiers: more than 20% (in the period 2009–2018 and in 2018 only, 30 and 38 stations, respectively), between 10 and 20% (8 and 4 stations,

Table 1. List of stations with their coordinates and sampling heights.

ID	station	country	lat [°]	lon [°]	alt [m.a.s.l.]	inlet [m.a.g.l.]
BIK	Białystok	Poland	53.2320	23.0270	183	5, 30, 90, 180, 300
BIR	Birkenes	Norway	58.3886	8.2519	219	2.5
BIS	Biscarrosse	France	44.3781	−1.2311	73	47
BRM	Beromünster	Switzerland	47.1896	8.1755	797	12, 45, 72, 132, 212
BSD	Bilsdale	UK	54.3590	−1.1500	380	42, 108, 248
CBW	Cabauw	The Netherlands	51.9710	4.9270	−1	27, 67, 127, 207
CMN	Monte Cimone	Italy	44.1667	10.6833	2165	8, 12
CRP	Carnsore Point	Ireland	52.1800	−6.3700	9	14
DEC	Delta de l'Ebre	Spain	40.7439	0.7867	1	10
EEC	El Estrecho	Spain	36.0586	−5.6640	20	20
ERS	Ersa	France	42.9692	9.3801	533	40
FKL	Finokalia	Greece	35.3378	25.6694	250	15
GAT	Gartow	Germany	53.0657	11.4429	70	30, 60, 132, 216, 341
GIC	Sierra de Gredos	Spain	40.3457	−5.1755	1436	20
HEI	Heidelberg	Germany	49.4170	8.6740	116	30
HPB	Hohenpeissenberg	Germany	47.8011	11.0246	934	50, 93, 131
HTM	Hyltemossa	Sweden	56.0976	13.4189	115	30, 70, 150
HUN	Hegyhatsal	Hungary	46.9500	16.6500	248	10, 48, 82, 115
IPR	Ispra	Italy	45.8147	8.6360	210	40, 60, 100
IZO	Izana	Spain	28.3090	−16.4990	2372.9	13
JFJ	Jungfraujoch	Switzerland	46.5500	7.9870	3570	10
KAS	Kasprowy Wierch	Poland	49.2325	19.9818	1989	5
KRE	Krešín u Pacova	Czech Republic	49.5830	15.0800	534	10, 50, 125, 250
LHW	Laegern-Hochwacht	Switzerland	47.4822	8.3973	840	32
LIN	Lindenberg	Germany	52.1663	14.1226	73	2.5, 10, 40, 98
LMP	Lampedusa	Italy	35.5300	12.5200	45	10
LMU	La Muela	Spain	41.5941	−1.1003	571	80
LUT	Lutjewad	The Netherlands	53.4036	6.3528	1	60
MHD	Mace Head	Ireland	53.3261	−9.9036	8	24
MLH	Malin Head	Ireland	55.3550	−7.3330	22	47
NOR	Norunda	Sweden	60.0864	17.4794	46	32, 59, 100
OHP	Obs. de Haute Provence	France	43.9310	5.7120	650	100
OPE	Obs. pérenne de l'environnement	France	48.5619	5.5036	390	10, 50, 120
PAL	Pallas	Finland	67.9733	24.1157	565	5, 12
PDM	Pic du Midi	France	42.9372	0.1411	2877	10, 28
PRS	Plateau Rosa	Italy	45.9300	7.7000	3480	10
PUI	Puijo	Finland	62.9096	27.6549	232	79, 84
PUY	Puy de Dôme	France	45.7719	2.9658	1465	10
RGL	Ridge Hill	UK	51.9976	−2.5000	204	45, 90
SAC	Saclay	France	48.7227	2.1420	160	15, 60, 100
SMR	Hyytiälä	Finland	61.8474	24.2947	181	16.8, 67.2, 125
SSL	Schauinsland	Germany	47.9200	7.9200	1205	12
SVB	Svartberget	Sweden	64.2560	19.7750	235	35, 85, 150
TAC	Tacolneston	UK	52.5170	1.1386	56	54, 100, 185
TRN	Trainou	France	47.9647	2.1125	131	5, 50, 100, 180
UTO	Utö	Finland	59.7839	21.3672	8	57

(*Continued.*)

Table 1. (*Continued.*)

ID	station	country	lat [°]	lon [°]	alt [m.a.s.l.]	inlet [m.a.g.l.]
WAO	Weybourne	UK	52.9500	1.1219	20	10
ZEP	Ny-Alesund	Norway	78.9067	11.8883	474	15
SOD	Sodankylä	Finland	67.367	26.631	188	total column

respectively) and less than 10% (10 and 6 stations, respectively). A total of 44 stations cover the growing season of the year 2018, with valid monthly means for all months from April to October. Out of these, 22 stations are located in an area affected by a 1.5-σ temperature anomaly, or more, compared to the 2009–2018 period, at least for one month in summer 2018, based on 0.25° gridded climate ERA5 reanalysis data [23].

3. Analysis of the atmospheric CO_2 seasonal cycle across Europe

We applied a data selection scheme to all time series in order to minimize the effects of local contributions, and increase the spatial representativeness of each record. Except for Mace Head (MHD), where we used a selection scheme based on wind speed, direction, and hourly standard deviation of CO_2 [24], we have applied a simple selection to all stations. It consists of retaining mid-afternoon (12–17 h local winter time) data at tall tower and coastal stations, and retaining night-time (20–05 h local winter time) data at mountain stations, when the air is well-mixed, providing a large spatial representativeness with minimum influence from local sources [15,25,26]. In addition to this temporal filtering we also excluded hourly means with a standard deviation greater than 0.5 ppm from the selected time series. As a consequence, this data selection significantly reduces the number of hourly averages (26% of the total), but only marginally affects the number of daily averages (by 5.5% on average). From the selected dataset, we have estimated the seasonal cycles of atmospheric CO_2 concentration by using the curve fitting procedure developed by Thoning *et al.* [27]. For each station, the CO_2 time series are fitted with a 4-harmonics curve and a quadratic polynomial function. Residuals from this fit are filtered in the time domain using a low-pass filter in order to separate high-frequency variations and inter-annual variabilities.

Figure 3 shows selected hourly measurements, as well as the corresponding smoothed curves from four tall tower sites: Hyltemossa (HTM, Sweden), Gartow (GAT, Germany), Tacolneston (TAC, UK) [28] and Observatoire Pérenne de l'Environnement (OPE, France) [29]. The smoothed curves are compared to the one inferred from the marine sector selection at Mace Head, which can be chosen as a marine background station for air masses advected into the European continent, a site commonly used as a background reference for Western Europe [1]. This comparison with MHD is only qualitative. Calculating the differences in concentrations between stations upstream and downstream from European sources would require a more detailed analysis of air mass trajectories, and the optimal background would probably be different depending on the European regions considered. The signals observed at these four stations are typical for rural sites. They are characterized by strong positive synoptic CO_2 events in the winter half-year from September to early March, when CO_2 concentration is at the higher part of its seasonal cycle. These episodes correspond to periods of low-atmosphere stratification, leading to an accumulation of gases emitted at the surface in the atmospheric boundary layer. In the case of CO_2, the emissions in the non-growing season originate from both anthropogenic and biogenic sources. This corresponds to the period with CO_2 concentrations at the European sites larger than marine background concentrations measured at Mace Head. By contrast, CO_2 concentrations at inland stations are lower than those at Mace Head from March to July, due to the influence of CO_2 absorption by European ecosystems, which dominates the continued anthropogenic emissions at the continental scale. Note that there is no symmetry between the amplitude of the winter peaks and the negative peaks of spring, mainly because of limited vertical development of the atmospheric boundary layer in autumn/winter [30,31] which amplifies the atmospheric signals measured at the surface during those seasons. Additionally, in winter both anthropogenic emissions and biogenic emissions contribute to positive synoptic anomalies, whereas in summer they mainly offset each other. Only clean air masses that did not receive recent anthropogenic emissions while being exposed to CO_2 uptake can create negative synoptic CO_2 anomalies [32–34].

Over the 2009–2018 period, we calculated the amplitude of the seasonal cycle as the difference between the smoothed monthly mean maximum in winter and the minimum in summer. The largest and smallest amplitude were observed at the urban site of Heidelberg (32 ppm), and at the background marine site of Izaña (7.8 ppm), respectively. In addition to its marine footprint, the smaller amplitude at the latter station is due to its location south of continental Europe. At Mace Head, the CO_2 amplitude for oceanic air masses is on average 14.9 ppm. Overall, we may distinguish between the coastal sites like Mace Head (12 sites), which display an average annual amplitude of 14.5 ± 3.0 ppm, the mountain sites (7 sites) with an amplitude of 12.4 ± 2.0 ppm, and the highest sampling levels of the tall towers (20 sites) with a mean amplitude of 21.0 ± 3.0 ppm. The higher seasonal amplitude observed at the tall towers, compared to the coastal and mountain sites, can be explained in part by a higher exposure to biospheric fluxes, but also by being subject to the greater dynamics of the continental boundary layer [31,35].

4. Atmospheric CO_2 concentrations fingerprint of the 2018 European summer climate anomaly

The climate anomaly in Europe during 2018 was characterized by temperatures higher than normal for every month from April to December, and by a sustained dry period from June to November in Central Europe, with a fast transition from normal to drought conditions from spring to late spring and

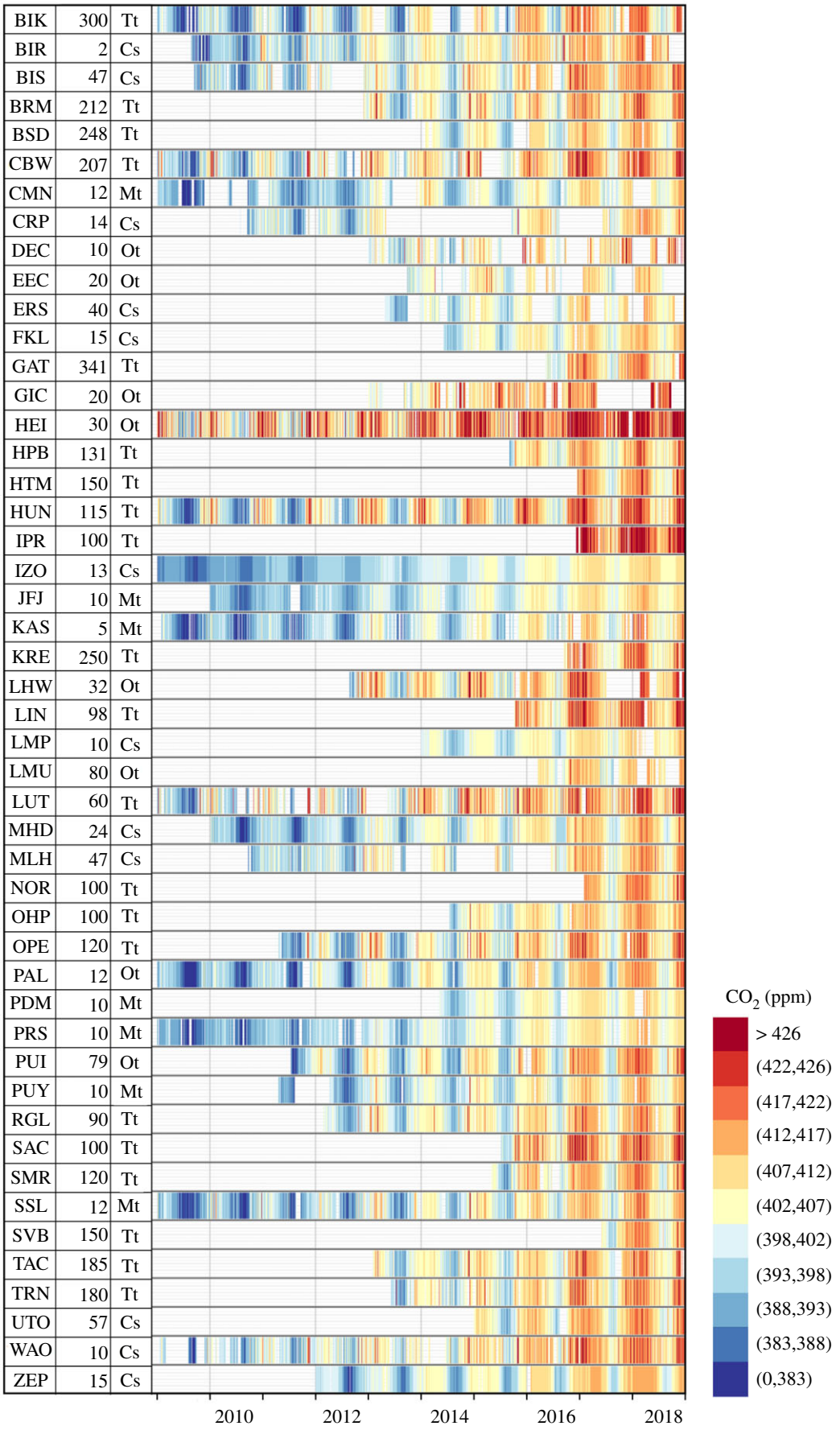


Figure 2. Time series of CO_2 mole fractions (ppm) at 48 sites in Western Europe over the period 2009–2018. Each vertical coloured line represents a CO_2 daily average. The second column indicates the sampling height above ground level, and the third column indicates whether the station is a tall tower (Tt), coastal (Cs), mountain (Mt) or other surface site (Ot). The colour code indicates the CO_2 mole fraction in ppm. (Online version in colour.)

summer [12,14,36]. Europe experienced late spring and summer temperatures that were more than 1°C warmer than 1981–2010 [37,38], with the highest temperature anomalies (+2.5°C) being observed in May–June. Most of Europe was affected, but the anomaly was particularly marked in Central and Northern Europe (electronic supplementary material,

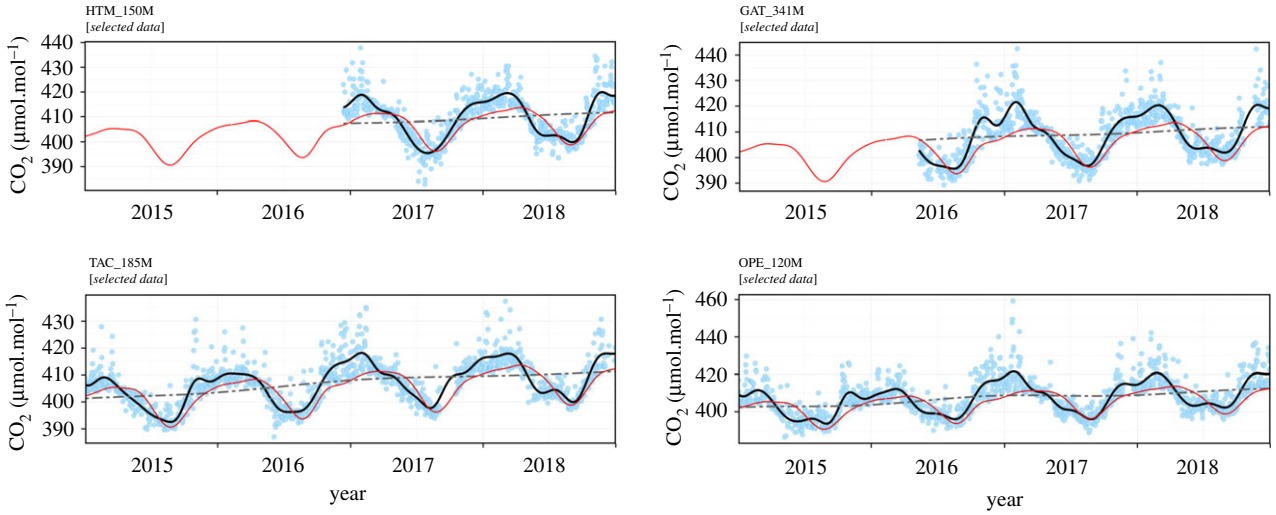


Figure 3. CO_2 time series observed at Hyltemossa (HTM, Sweden), Gartow (GAT, Germany), Tacolneston (TAC, UK) and Observatoire Pérenne de l'Environnement (OPE, France). Each blue dot corresponds to a daily average, after data selection as described in the main text. The black curve shows the smoothed curve of these points, and the dash-dot line the long-term trends. The red curve represents the smooth curve of the CO_2 time series at Mace Head, Ireland, in the marine sector. (Online version in colour.)

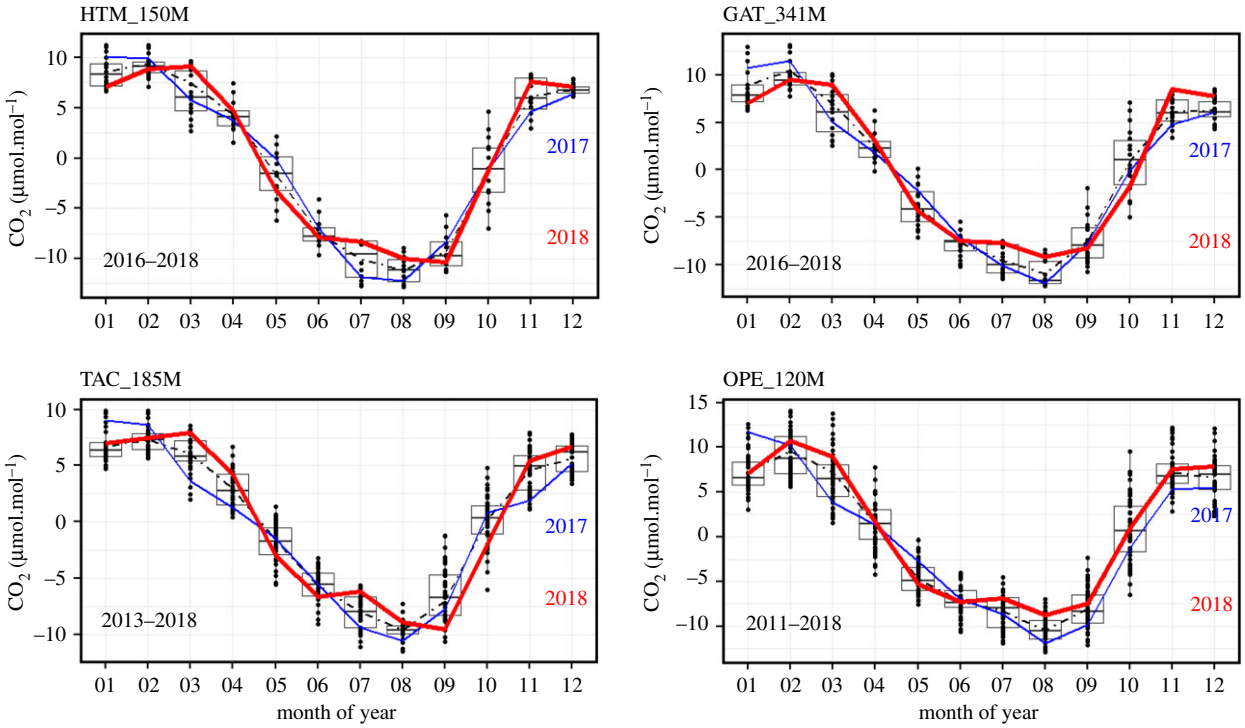


Figure 4. CO_2 seasonal cycles observed at Hyltemossa (HTM, Sweden), Gartow (GAT, Germany), Tacolneston (TAC, UK) and Observatoire Pérenne de l'Environnement (OPE, France). The 2018 cycle is shown in red, 2017 in blue, and a statistical summary of the full measurement period as box-and-whisker plots showing the median, first and third quartiles over the entire measurement period of each station, indicated in the bottom left corners of the plots. Corresponding figures for all other stations are shown in electronic supplementary material, figure S2. (Online version in colour.)

figure S1). In Southern Europe, particularly the Iberian Peninsula, the conditions in summer and spring were wetter than usual and likely promoted stronger biospheric CO_2 uptake. In this region, crop yields were found to be higher than normal during 2018, whereas low and extremely low yields were recorded in Central and Northern Europe [12,39].

The atmospheric CO_2 seasonal cycle observed at the top level of four tall towers located in the UK, France, Germany and Sweden, were clearly affected by the drought in 2018 (figure 4). For all four sites, we observe a similar pattern during the summer of 2018. While the overall pattern compares well with previous years, the CO_2 drawdown, normally observed between March and August, was reduced between June and August 2018. In comparison with the average of the previous years (see the periods in figure 4), the occurrence of the daily concentration minimum in summer 2018 was delayed by 12, 13, 28 and 32 days for OPE, GAT, TAC and HTM, respectively. For these four sites, the mean CO_2 anomaly (2018 minus the average of previously available years) was 1.7 ± 0.2 ppm and 1.3 ± 0.5 ppm in July and August, respectively, which corresponds to 17% and 12% of the mean CO_2 drawdown (defined as the annual minimum value). Figure 5 shows the mean CO_2 anomaly for all the sites whose data are part of this analysis. Among the 20 tall towers, only

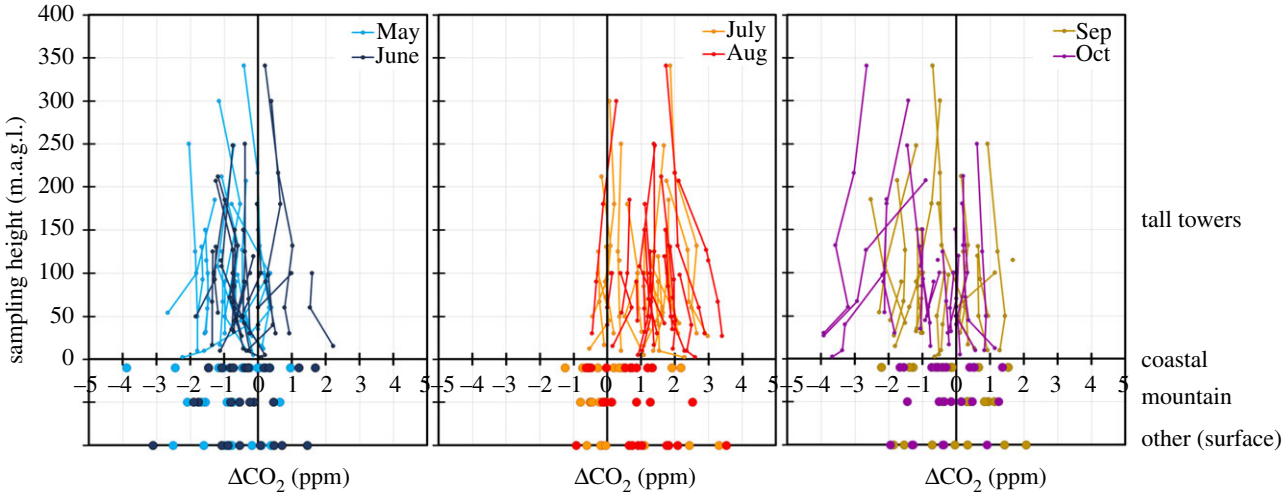


Figure 5. Monthly mean CO_2 differences anomalies for each month during May to October 2018, compared to the same month during previous years, the data being available from 2009 to 2018 with variable coverage between stations, i.e. CO_2 (2018) minus CO_2 (previous years). Upper panel shows the vertical profile of tall towers, whereas the bottom panel shows separately coastal, mountain and other surface sites. (Online version in colour.)

a few did not see a positive anomaly during the months of July and August (BRM, Switzerland; HPB, Germany; IPR, Italy, in July; and BIK, Eastern Poland, in August). The average concentration anomaly in July–August, taking into account the 20 tall towers (highest sampling levels), is 0.9 ± 0.8 ppm in July, and 1.3 ± 0.7 ppm in August. It is significantly lower at the seven mountain sites (−0.4 and +0.6 ppm in July and August, respectively), as they are less exposed to regional scale vegetation-atmosphere CO_2 exchange (electronic supplementary material figure S2). From our analysis, we conclude that nearly all stations located on the European continent show reduced CO_2 seasonal amplitudes from spring to late summer in 2018 compared to 2017. Because fossil fuel CO_2 emissions were similar in these 2 years across European countries [40,41], this anomaly must reflect a weaker net CO_2 uptake during this period, possibly coupled with weather-related atmospheric CO_2 enrichment. Four types of weather regimes (NAO+, NAO−, blocking and Atlantic ridge) are generally defined by classifying the geopotential height anomalies at 500 hPa [42–44]. There are clear spatial patterns of precipitation and temperature associated with these regimes: for example, drought periods in Scandinavia and Central Europe are closely correlated with blocking regimes [43]. In July/August 2018, based on NCEP reanalysis data, we classified 26, 22, 13, 1 days as Atlantic Ridge, blocking, NAO+ and NAO− regimes, respectively. This compares with an average of 13, 14, 18, 17 days on average for the period 2009–2017. The July–August period of 2018 saw an increase in the number of days where European weather conditions were dominated by Scandinavian blocking regimes compared to the average (22 versus 14). Conversely, there were far fewer NAO− regime days in 2018 (1 versus 17.1), which are associated with colder and wetter weather in Western and Northern Europe [45]. Both the relatively high number of blocking days, and low number of NAO+ days indicate lower-than-average surface wind speeds in Western and Northern Europe. On the one hand, this suggests that part of the anomaly in atmospheric CO_2 concentrations may have been due to an anomaly of the wind patterns, which reduced, e.g. the dispersion of CO_2-enriched air from anthropogenic sources, in addition to any perturbation of biogenic CO_2 fluxes. An estimate of this contribution from atmospheric transport could be made using atmospheric circulation tracers, such as Radon-222. On the other hand, the atmospheric transport contribution is taken into account in the atmospheric inversions described in this special issue, concluding a reduction of the biospheric CO_2 uptake by 20–30% in Western, Central and North Europe [15].

It is also noticeable that lower than average CO_2 concentrations in spring and autumn 2018 (figure 5) were observed at most measurement sites. This difference in CO_2 concentration is -0.7 ± 0.6 and -1.3 ± 0.9 ppm for the months of May and September 2018 if we only consider the 10 stations located in the area where the mean temperature anomaly in summer is larger than 1.5 σ of the 2009–2018 average (values are -0.8 ± 0.7 and -0.4 ± 1.1 ppm, respectively, in May and September when considering all tall towers). The negative difference in spring is likely related to an earlier onset of the growing season and enhanced photosynthesis, promoted by extremely warm conditions and increased solar radiation [12,14]. In autumn, the negative differences in CO_2 concentration may reflect either a prolonged growing season, as temperatures remained high, but also possibly a reduction in respiration due to summer productivity collapse. The results discussed above were obtained from atmospheric CO_2 concentrations selected during daytime for all lowland stations, when the atmospheric boundary layer is well developed. Night-time measurements have a significantly reduced footprint due to the lower atmospheric mixing, and they are not used in atmospheric inversions that have trouble representing the night-time boundary layer. We, therefore, analysed the CO_2 diurnal cycles by calculating each day the difference of the night-time concentrations (01–05 h LT) compared to daytime values (12–16 h LT). From the four tall towers shown in figure 6, those differences oscillate between values close to 0 in winter, and maximum values (2–10 ppm) in May–June. The purpose of this analysis is mainly to verify if the amplitude of the diurnal cycles has been modified in 2018 compared to previous years. The 2018 anomaly of this signal is represented on the bottom panel of figure 6. In general, there is an increase in the amplitude of the diurnal cycle in spring, and a decrease in summer. The closer you get to the surface, the more amplified this signal is due to the stronger influence of surface sources in the towers' footprints. Overall, looking at the tall towers located in the area the most affected by the drought

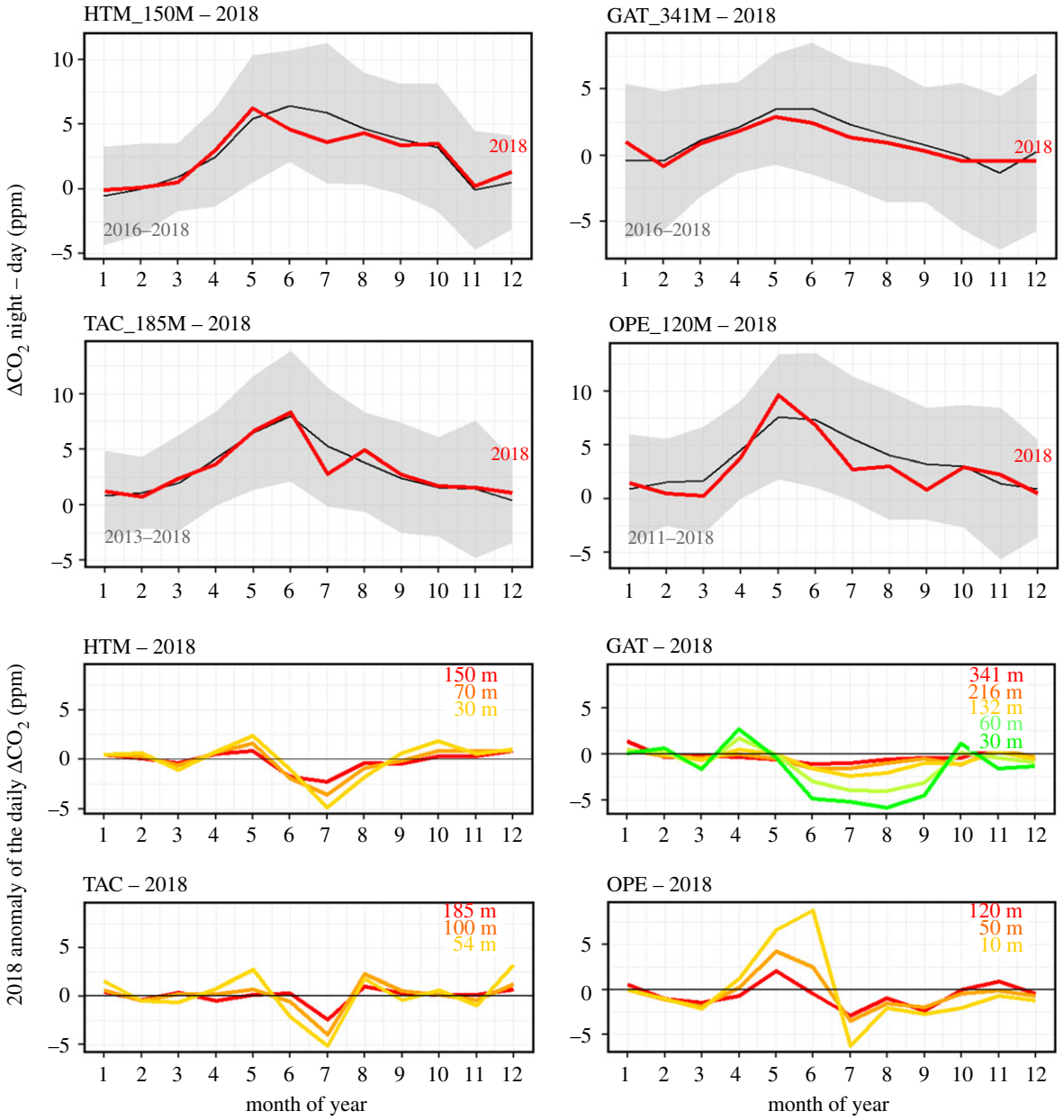


Figure 6. The top panel shows, at four tall towers (highest levels), the amplitude of the CO_2 daily cycles averaged every month for all available years (black line and grey area), and for 2018 (red line). The bottom panel shows, for the same sites, the differences of CO_2 daily cycles between 2018 and the average over all available years. The colours represent the different sampling levels at the towers (red curves correspond to the top panel figures). (Online version in colour.)

(12 sites), the average amplitude of the daily cycle observed at elevation greater or equal to 100 m a.g.l., is increased by 0.4 ± 0.9 ppm in May 2018, and reduced by −2.0 ± 0.8 ppm in July 2018. For the same sites, if we select only observations below 100 m.a.g.l. the 2018 anomaly is 1.1 ± 2.9 ppm in May and −3.4 ± 2.0 ppm in July. The reduction of the CO_2 daily amplitude in July can be due to an increase of the daytime concentrations associated with the reduction of the surface uptake by ecosystems, and/or a decrease of night-time concentrations. Considering that these values are greater than the anomaly calculated solely from afternoon data, it seems that this signal points to a significant contribution of ecosystem respiration, which is also the conclusion from observations at ICOS eddy-covariance sites [14].

We have applied the same analysis to the column-averaged dry air mole fractions of CO_2 (XCO_2) observations at the TCCON (total carbon column observing network) site of Sodankylä (referred to as SOD in table 1) in northern Finland, where measurements have been made since 2009 [46,47]. Compared

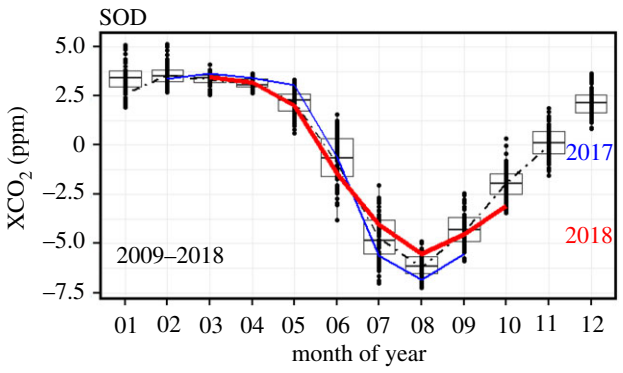


Figure 7. Same as figure 4 but for the column-averaged dry air mole fraction of CO_2 (XCO_2) measured at the TCCON site of Sodankylä, Finland. (Online version in colour.)

to the surface measurements, the amplitude of the seasonal cycle of XCO_2 measurements is smaller (9.8 ppm on average). This is due to the fact that the column-averaged mole fraction

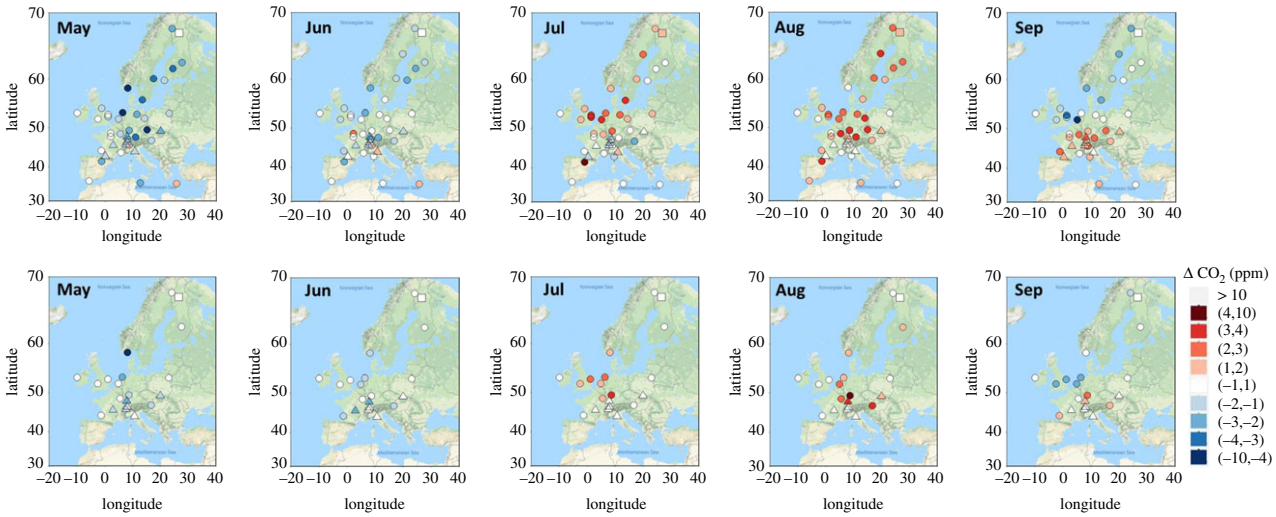


Figure 8. Map of the monthly mean CO_2 differences (2018 minus 2017) from May (left) to September (right). Circles represent surface stations in lowlands. Triangles indicate the mountain sites, and the square indicates a total column measurement station (TCCON). Top panels show the differences for 2018 minus 2017. Bottom panels show differences for 2018 minus 2010–2017 mean. (Online version in colour.)

is almost insensitive to vertical transport. But nevertheless, the minimum monthly XCO_2 also occurs in August due to the uptake of carbon into the biosphere [46] at this TCCON site. The time series of the XCO_2 and discussion about the specific data handling is given in electronic supplementary material, figure S3. In 2018, we observed a similar pattern for XCO_2 compared to the surface stations, with higher concentrations in July and August by +0.8 and +0.6 ppm, whereas, the difference in XCO_2 concentration is 0.3 and −0.2 ppm for the months of May and September 2018 (figure 7; electronic supplementary material, figure S4). The missing values from November until January are normal for this latitude, as the sun is at a very high zenith angle in the sky and the data are filtered following the TCCON recommendations.

The average CO_2 differences deduced from the measurement network mask regional disparities, because the 2018 drought was not uniform throughout the European continent [12,14]. In order to visualize the regional patterns of the atmospheric CO_2 anomaly, we mapped the detrended CO_2 differences observed from May to September 2018 compared to the previous year (figure 8, top panel plots), and compared to the average of the eight previous years where data are available since 2010 (figure 8, bottom panel plots). The first comparison benefits from the very recent development of the measurement network which allows a representation of CO_2 concentrations with a high density of measurement points, while the second makes it possible to compare the measurements of 2018 with an average over a more representative period. Figure 8, top panel plots clearly shows the development of a positive CO_2 difference (2018–2017) of around 2 to 4 ppm in July/August in the central and northern part of Europe. For the northern part of Europe (UK, Benelux, northern Germany and Scandinavia), the CO_2 differences between 2018 and 2017 switch to negative values (−2 to −4 ppm) in September/October. However, this is not the case for stations located further south, where the 2018–2017 differences remain positive. When looking at the sites with longer time series (figure 8, bottom panel plots), this latter signal goes very close to zero, which is not the case for the positive/negative signals observed in the Northern part of Europe.

5. Comparison of the 2018 climate anomaly with previous European droughts

Due to the relatively recent expansion of the monitoring network, it is difficult to compare the signals observed in summer 2018 with previous drought events. In addition, the geographical extension of the droughts recorded in Europe in 2003, 2015 and 2018 do not overlap, therefore not all the same stations have been affected [13,36]. However, it remains possible to compare the amplitudes of the CO_2 anomalies observed in 2018 and during previous droughts in 2003 and 2015. The heatwave of 2003 had dramatic health consequences in Western Europe, and in terms of carbon cycle, Ciais *et al*. [48] estimated a 30% reduction in gross primary productivity over Europe, which resulted in a strong anomalous net source of carbon dioxide (0.5 Pg C) to the atmosphere. This study was based on ecosystem observations and models but did not use information provided by the limited existing atmospheric CO_2 records. Compared to 2018, the 2003 drought was more centred on Western and Southern Europe [48]. The dataset compiled as part of this study includes eight stations from the most affected region in 2003 (electronic supplementary material, figure S5). Five of them are located in an area significantly affected by the heat wave of August 2003 (anomaly of the mean temperature greater than 1.5 σ of the 2009–2018 average). Among these five stations, one (CBW) provided no data from 17 June to 15 August 2003, and is therefore not taken into account in the present analysis. At the other four stations, the CO_2 concentration anomaly is greater than 2 ppm (4.5 ppm at SSL, 2.1 ppm at CMN, 2.7 ppm at HUN, 2.6 ppm at HEI) in 2018, and the average anomaly is $+3.0 \pm 1.1$ ppm in August 2003 (figure 9; electronic supplementary material, figure S5). In July 2018, for comparison, if we exclude the 12 coastal/oceanic stations, ten stations out of a total of 36 are located in a temperature anomaly zone following the same criterion (greater than 1.5 σ of the 2009–2018 average). The average CO_2 anomaly of those ten sites in July and August 2018 is $+1.3 \pm 0.4$ ppm and $+1.4 \pm 0.5$ ppm, respectively. It is interesting to note that both in 2003 and 2018, the

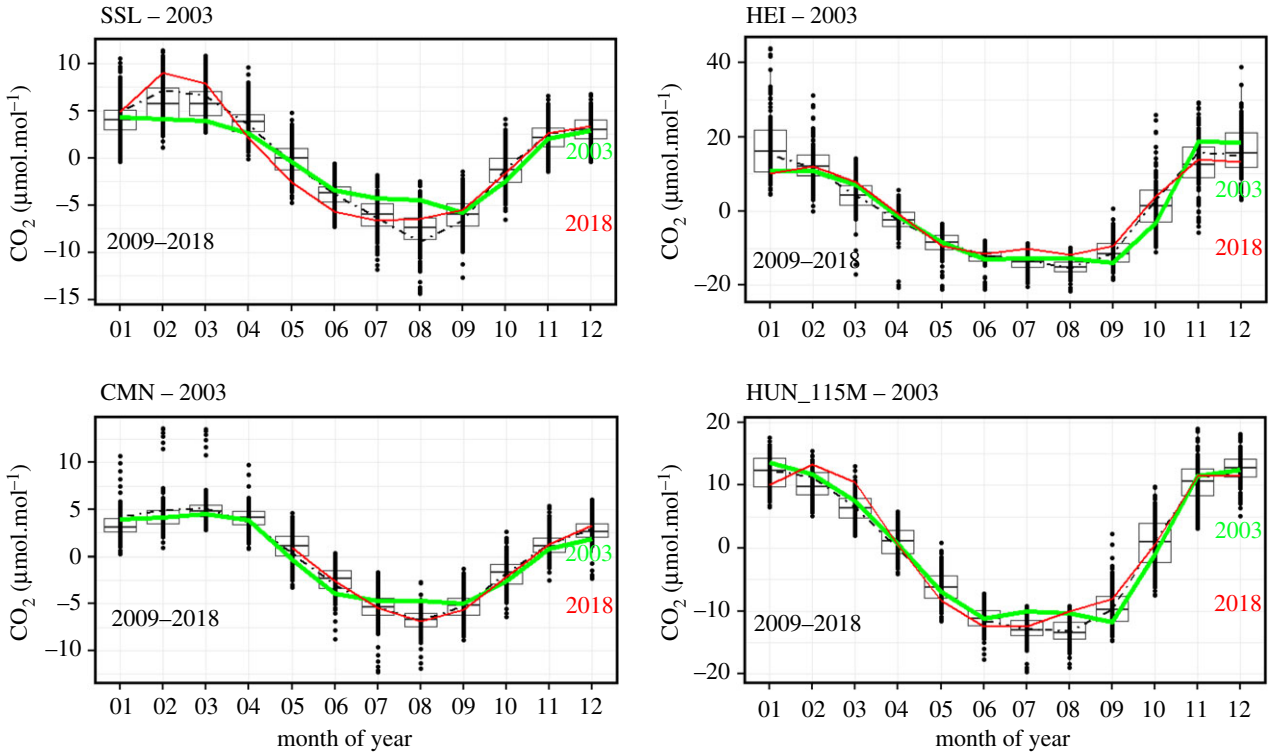


Figure 9. Same as figure 4 for the 2003 (green) and 2018 (red) seasonal cycles at Shauinsland (SSL, Germany), Heidelberg (HEI, Germany), Monte Cimone (CMN, Italy) and Hegyhatsall (HUN, Hungary). (Online version in colour.)

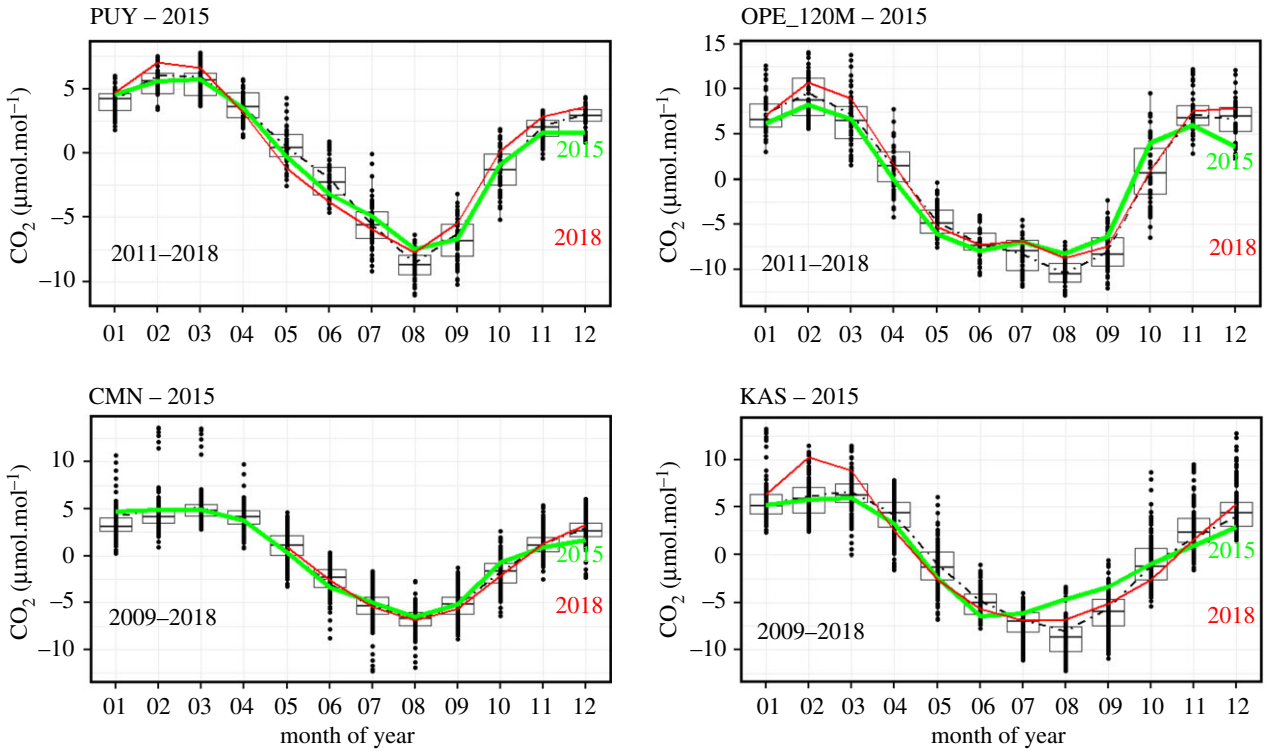


Figure 10. Same as figure 4 for the 2015 (green) and 2018 (red) seasonal cycles at Puy de Dôme (PUY, France), Observatoire Pérenne de l'Environnement (OPE, France), Monte Cimone (CMN, Italy), Kasprowy (KAS, Poland). (Online version in colour.)

atmospheric CO_2 records indicate a reduction of the CO_2 uptake in summer associated with the droughts, but, on the contrary, an apparent increase of the uptake in the preceding spring and following autumn. The year 2018 was characterized by an early heatwave in spring, with moderate rainfall deficits, providing favourable conditions for the vegetation growth and carbon uptake [12]. As demonstrated by recent studies [12,49], such conditions favour the reduction of soil moisture in summer due to greater evapotranspiration. In spring 2018, the CO_2 anomaly averaged over the ten stations located in the drought zone is -0.7 ± 0.6 ppm in May 2003, and is -0.3 ± 0.7 ppm (4 sites) in June 2003. Similarly, the autumn CO_2 anomaly in 2018, associated with the mild climate, reaches -1.3 ± 0.6 ppm in September 2018 (10 sites)

(figures 4, 5 and 8), and -2.6 ± 2.5 ppm in October 2003 (4 sites) (figure 9; electronic supplementary material, figure S5).

The temperature anomaly in summer 2015 mainly affected Southern Europe in July, and Central Europe in August. Only two CO_2 stations in Poland were located in the heart of the temperature anomaly in August 2015, and CO_2 anomalies of +0.4 and +3.4 ppm were observed at BIK and KAS, respectively (figure 10; electronic supplementary material, figure S5). In July, 11 of the 29 non-coastal stations measuring in 2015 were located in the temperature anomaly area (greater than 1.5 σ of the 2009–2018 average). The CO_2 anomaly recorded by these stations was on average +1.0 ± 0.6 ppm (electronic supplementary material, figure S5). The CO_2 anomaly observed in the summer of 2015 at stations in Southern Europe had, therefore, less impact on the biospheric uptake than in 2003 and 2018, and no significant negative anomaly is observed in spring and autumn.

6. Conclusion

In the context of the 2018 drought study, we have merged the largest ever dataset on atmospheric CO_2 concentrations in Europe with 48 measurement sites, including 20 tall towers sampling air at several levels above the ground. This dataset, made available via the ICOS Carbon Portal (doi:10.18160/ere9-9d85), goes well beyond the 2018 drought study, since it includes the historical measurement series of the involved stations. It has already been used in three atmospheric inversions aiming to determine the impact of the 2018 drought on CO_2 exchanges with terrestrial ecosystems [13–15]. The objective of this study was to characterize the anomaly of CO_2 concentrations observed over the European continent in 2018, and to compare it with previous droughts. Taking into account the sites located in the areas most affected by the 2018 drought [12], in Central and Northern Europe, it appears that the seasonal minimum of CO_2 in summer (July–August) has been reduced by 1.4 ± 0.5 ppm (12% of the seasonal minimum). It is difficult to compare the impact of different droughts with each other because of the geographical diversity of these droughts, as well as the smaller number of stations available in the past. However, by selecting stations located in areas where temperature anomalies are at least 1.5 σ relative to climatology, the impact of the 2018 drought on CO_2 concentrations is found to be between those of 2003 (3.0 ± 1.1 ppm) and 2015 (1.0 ± 0.6 ppm). It should be noted that the apparent decrease in carbon absorption in the summer of 2018 appears to be partially offset by an apparent higher absorption in the spring and autumn of the same year. Making the difference in this atmospheric signal between the contributions of atmospheric transport (droughts are accompanied by an increase in anticyclonic blocking conditions) and the different components of the biospheric fluxes (gross primary productivity, ecosystem respiration, biomass burning) remains a difficult challenge. To go further in the interpretation, we will have to use other types of datasets. Satellite observations can complement surface measurements to better characterize spatial variability. Recent studies have demonstrated the possibility of detecting seasonal XCO_2 signals related to the growing or fire seasons, and to use tropospheric NO_2 columns as an indicator of anthropogenic pollution plumes [50]. However, considering the intensity of the signals measured at the surface during the 2018 drought (less than 2 ppm), obtaining sufficiently precise measurements from space remains a challenge in view of the performance of current sensors [51]. Another promising axis for the interpretation of CO_2 measurements is to develop the use of atmospheric compounds, such as CO, CH_4, Radon-222, COS and isotopes. The correlations of these compounds with CO_2 will provide information allowing, for example, normalization of the influence of the large-scale atmospheric circulation in Europe that affects all atmospheric compounds, or quantification of the intensity of biomass burning (e.g. CO, black carbon). For this purpose, the establishment of a dense network of atmospheric observatories in Europe, dedicated to multi-compound measurements and anchored in the long term (thanks to research infrastructures such as ICOS and ACTRIS) is essential to improve our understanding of the impact on our environment of extreme events, such as droughts and heatwaves, likely to intensify in the decades to come.

Data accessibility. Atmospheric CO_2 data from the 48 surface stations are available at the ICOS Carbon Portal (https://www.icos-cp.eu/): doi:10.18160/ere9-9d85. Total column data from SOD station are available at the TCCON server (https://tccon-wiki.caltech.edu/Network_Policy/Data_Use_Policy).

Authors' contributions. M.Ra. led the authoring team and analyses; P.Ci. and A.Ba. contributed to the data analysis, and the relation with climate anomaly; L.Ha., K.Ya. and L.Ri. contributed to the data processing; M.K.Sh. contributed to total column analysis; A.Re. contributed to the weather regimes analysis; and following co-authors contributed to the atmospheric observations: C.Ge. and J.V.La. for BIK; M.De. and M.Ra. for stations in France; C.L.My. and O.He. for BIR, ZEP; M.Le. for BRM; S.O'Do. and K.St. for BSD, RGL, TAC; A.Fr. A.He. and A.Ve. for CBW; L.C.d.T. and P.Cr. for CMN; D.Ma. for CRP, MLH, MHD; R.Cu., J.A.Mo. and X.Ro. for DEC, EEC, GIC, LMU; C.Ph. for ERS; N.Mi. for FKL; D.Ku., M.Li., C.P.Du. and D.We. for GAT, HPB, LIN; S.Ha. and I.Le. for HEI; M.He. for HTM; L.Ha. for HUN; P.Be. and G.Ma. for IPR; E.Cu. for IZO; L.Em. and M.St. for JFJ; J.Ba., L.Ch. and J.Ne. for KAS; K.Ko., G.Vi. and M.V.Ma. for KRE; D.Br. and S.He. for LHW; A.di.Sa., S.Pi. and D.Sf. for LMP; H.Ch. and H.A.Sc. for LUT; I.Le. and M.Ot. for NOR; P-E.Bl. and I.X.R. for OHP; S.Co. and O.La. for OPE; J.Ha. and T.La. for PAL, PUI, UTO; F.Gh. for PDM; F.Ap., F.Ca. and P.Tr. for PRS; A.Le. and K.E.J.Le for PUI; A.Co., JM.Pi. and C.Y.K. for PUY; P.Ke. and I.Ma. for SMR; F.Me. for SSL; P.Ma. and M.Ot. for SVB; M.Lo. for TRN; G.Fo. and A.Ma. for WAO; R.Ki. and K.M.Sh. for SOD.

Competing interests. We declare we have no competing interests.

Funding. The UK sites were funded by the UK Department of Business, Energy and Industrial Strategy (formerly the Department of Energy and Climate Change) through contracts TRN1028/06/2015 and TRN1537/06/2018. The Cabauw measurements have been supported by the Dutch government as well as national and European projects. The Hegyhatsall measurements have been supported by the Hungarian Meteorological Service, and funded by the project OTKA K129118. For Bialystok, we wish to acknowledge the support of the Max Planck Society and AeroMeteo Service Krzysztof Katryński. Operation of the Krešín u Pacova station was supported by the Ministry of Education, Youth and Sports of CR within the CzeCOS program, grant number LM2015061 and within the National Sustainability Program I (NPU I), grant number LO1415. Measurements at Lampedusa were supported by the Italian Ministry for University and Research through project NextData and the ICOS-Italy Joint Research Unit. The stations at the ClimaDat Network in Spain have received funding from the 'la Caixa' Foundation, under agreement 2010-002624.

Acknowledgements. The authors acknowledge all the technical staff in charge of operating the atmospheric stations. ICOS activities at CMN have been implemented by the National Project of Interest NextData and are supported by the Ministry of Education, University and Research and by the 'ICOS-Italy' JRU; CNR acknowledges the

logistic support and hospitality of Italian Air Force 'CAMM'. Thanks to the people from the Parc Científic de Barcelona (PCB-UB), the Catalan Institute of Climate Sciences (IC3) and the Institut de Ciència i Tecnologia Ambientals (ICTA-UAB) who contributed to ClimaDat: MA Rodríguez-Arias, A Font, I Pouchet, A Águeda, R Arias, L Sánchez, P Occhipinti, M Tello, S Liñan, Ò Batet, M Nofuentes, C Grossi, M Ealo, S Borrás, L Cañas, E Vázquez, A Jornet, À Garriga, C Estruch. The French monitoring network acknowledges the long-term support received as part of the Service National d'Observation program. Thanks to V Legendre, P Wiszniowski, L Gest, PY Quéhé, J Helle, T Laemmel, L Vialettes, A Orgun, R Jacob, D Combaz, C Lett, O Llido, C Peureux, C Vuillemin, F Truong, B Gal.

References

1. Ramonet M *et al.* 2010 A recent build-up of atmospheric CO_2 over Europe. Part 1: observed signals and possible explanations. *Tellus B* **62**, 1–13. (doi:10.1111/j.1600-0889.2009.00442.x)
2. Conway TJ, Tans PP. 1999 Development of the CO_2 latitude gradient in recent decades. *Global Biogeochem. Cycles* **13**, 821. (doi:10.1029/1999GB900045)
3. Dlugokencky EJ *et al.* 2009 Observational constraints on recent increases in the atmospheric CH_4 burden. *Geophys. Res. Lett.* **36**, L18803. (doi:10.1029/2009gl039780)
4. Miller JB, Gatti LV, d'Amelio MTS, Crotwell AM, Dlugokencky EJ, Bakwin P, Artaxo P, Tans PP. 2007 Airborne measurements indicate large methane emissions from the eastern Amazon basin. *Geophys. Res. Lett.* **34**, L10809. (doi:10.1029/2006gl029213)
5. Ciais P, Rayner P, Chevallier F, Bousquet P, Logan M, Peylin P, Ramonet M. 2010 Atmospheric inversions for estimating CO_2 fluxes: methods and perspectives. *Clim. Change* **103**, 69–92. (doi:10.1007/s10584-010-9909-3)
6. Bergamaschi P *et al.* 2015 Top-down estimates of European CH_4 and N_2O emissions based on four different inverse models. *Atmos. Chem. Phys.* **15**, 715–736. (doi:10.5194/acp-15-715-2015)
7. Chevallier F, Remaud M, O'Dell CW, Baker D, Peylin P, Cozic A. 2019 Objective evaluation of surface- and satellite-driven CO_2 atmospheric inversions. *Atmos. Chem. Phys. Discuss.* **2019**, 1–28. (doi:10.5194/acp-2019-213)
8. Kountouris P, Gerbig C, Rödenbeck C, Karstens U, Koch TF, Heimann M. 2018 Atmospheric CO_2 inversions on the mesoscale using data-driven prior uncertainties: quantification of the European terrestrial CO_2 fluxes. *Atmos. Chem. Phys.* **18**, 3047–3064. (doi:10.5194/acp-18-3047-2018)
9. Gurney KR *et al.* 2003 TransCom 3 CO_2 inversion intercomparison: 1. Annual mean control results and sensitivity to transport and prior flux information. *Tellus Ser. B Chem. Phys. Meteorol.* **55**, 555–579. (doi:10.3402/tellusb.v55i2.16728)
10. Broquet G *et al.* 2013 Regional inversion of CO_2 ecosystem fluxes from atmospheric measurements: reliability of the uncertainty estimates. *Atmos. Chem. Phys.* **13**, 9039–9056. (doi:10.5194/acp-13-9039-2013)
11. Berchet A, Pison I, Chevallier F, Bousquet P, Bonne JL, Paris JD. 2015 Objectified quantification of uncertainties in Bayesian atmospheric inversions. *Geosci. Model Dev.* **8**, 1525–1546. (doi:10.5194/gmd-8-1525-2015)
12. Bastos A *et al.* 2020 Impacts of extreme summers on European ecosystems: a comparative analysis of 2003, 2010 and 2018. *Phil. Trans. R. Soc. B* **375**, 20190507. (doi:10.1098/rstb.2019.0507)
13. Rödenbeck C, Zaehle S, Keeling R, Heimann M. 2020 The European carbon cycle response to heat and drought as seen from atmospheric CO_2 data for 1999–2018. *Phil. Trans. R. Soc. B* **375**, 20190506. (doi:10.1098/rstb.2019.0506)
14. Smith NE *et al.* 2020 Spring enhancement and summer reduction in carbon uptake during the 2018 drought in northwestern Europe. *Phil. Trans. R. Soc. B* **375**, 20190509. (doi:10.1098/rstb.2019.0509)
15. Thompson RL *et al.* 2020 Changes in net ecosystem exchange over Europe during the 2018 drought based on atmospheric observations. *Phil. Trans. R. Soc. B* **375**, 20190512. (doi:10.1098/rstb.2019.0512)
16. WMO-GAW. 2012 *16th WMO/IAEA meeting on carbon dioxide, other greenhouse gases and related tracers measurement techniques (GGMT-2011), Wellington, New Zealand* (ed. G Brailsford). Geneva, Switzerland: WMO.
17. Zhao CL, Tans PP. 2006 Estimating uncertainty of the WMO mole fraction scale for carbon dioxide in air. *J. Geophys. Res. Atmos.* **111**, D08S09. (doi:10.1029/2005JD006003)
18. Cooperative Global Atmospheric Data Integration Project. 2018 Multi-laboratory compilation of atmospheric carbon dioxide data for the period 1957–2017; obspack_co2_1_GLOBALVIEWplus_v4.1_2018-10-29 [data set]. Boulder, CO: NOAA Earth System Research Laboratory, Global Monitoring Division.
19. Artuso F, Chamard P, Piacentino S, Sferlazzo DM, De Silvestri L, di Sarra A, Meloni D, Monteleone F. 2009 Influence of transport and trends in atmospheric CO_2 at Lampedusa. *Atmos. Environ.* **43**, 3044–3051. (doi:10.1016/j.atmosenv.2009.03.027)
20. Hazan L, Tarniewicz J, Ramonet M, Laurent O, Abbaris A. 2016 Automatic processing of atmospheric CO_2 and CH_4 mole fractions at the ICOS Atmosphere Thematic Centre. *Atmos. Meas. Tech.* **9**, 4719–4736. (doi:10.5194/amt-9-4719-2016)
21. Kwok CY *et al.* 2015 Comprehensive laboratory and field testing of cavity ring-down spectroscopy analyzers measuring H_2O, CO_2, CH_4 and CO. *Atmos. Meas. Tech.* **8**, 3867–3892. (doi:10.5194/amt-8-3867-2015)
22. Tans PP, Crotwell AM, Thoning KW. 2017 Abundances of isotopologues and calibration of CO_2 greenhouse gas measurements. *Atmos. Meas. Tech.* **10**, 2669–2685. (doi:10.5194/amt-10-2669-2017)
23. Copernicus Climate Change Service (C3S). 2017 ERA5: Fifth generation of ECMWF atmospheric reanalyses of the global climate Copernicus Climate Change Service Climate Data Store (CDS). See https://cds.climate.copernicus.eu/cdsapp#!/home.
24. Biraud S, Ciais P, Ramonet M, Simmonds P, Kazan V, Monfray P, O'Doherty S, Spain TG, Jennings SG. 2000 European greenhouse gas emissions estimated from continuous atmospheric measurements and radon 222 at Mace Head. Ireland. *J. Geophys. Res. Atmos.* **105**, 1351–1366. (doi:10.1029/1999JD900821)
25. Geels C *et al.* 2007 Comparing atmospheric transport models for future regional inversions over Europe – Part 1: mapping the atmospheric CO signals. *Atmos. Chem. Phys.* **7**, 3461–3479. (doi:10.5194/acp-7-3461-2007)
26. Gerbig C, Körner S, Lin JC. 2008 Vertical mixing in atmospheric tracer transport models: error characterization and propagation. *Atmos. Chem. Phys.* **8**, 591–602. (doi:10.5194/acp-8-591-2008)
27. Thoning KW, Tans PP, Komhyr WD. 1989 Atmospheric carbon dioxide at Mauna Loa Observatory, 2, analysis of the NOAA GMCC data, 1974, 1985. *J. Geophys. Res.* **94**, 8549–8565. (doi:10.1029/JD094iD06p08549)
28. Stanley KM *et al.* 2018 Greenhouse gas measurements from a UK network of tall towers: technical description and first results. *Atmos. Meas. Tech.* **11**, 1437–1458. (doi:10.5194/acp-2018-839)
29. Conil S, Helle J, Langrene L, Laurent O, Ramonet M. 2019 Continuous atmospheric CO_2, CH_4 and CO measurements at the OPE station in France from 2011 to 2018. *Atmos. Meas. Tech.* **12**, 6361–6383. (doi:10.5194/amt-12-6361-2019)
30. Pal S, Lopez M, Schmidt M, Ramonet M, Gibert F, Xueref-Remy I, Ciais P. 2015 Investigation of the atmospheric boundary layer depth variability and its impact on the Rn-222 concentration at a rural site in France. *J. Geophys. Res. Atmos.* **120**, 623–643. (doi:10.1002/2014jd022322)
31. Koffi EN *et al.* 2016 Evaluation of the boundary layer dynamics of the TM5 model over Europe. *Geosci. Model Dev.* **9**, 3137–3160. (doi:10.5194/gmd-9-3137-2016)
32. Aulagnier C, Rayner P, Ciais P, Ramonet M, Rivier L, Vautard R. 2010 Is the recent build-up of atmospheric CO_2 over Europe reproduced by models: an overview with the atmospheric mesoscale

transport model CHIMERE. *Tellus B* **62**, 14–25. (doi:10.1111/j.1600-0889.2009.00443)
33. Karstens U, Gloor M, Heimann M, Rodenbeck C. 2006 Insights from simulations with high-resolution transport and process models on sampling of the atmosphere for constraining midlatitude land carbon sinks. *J. Geophys. Res.* **111**, D12301. (doi:10.1029/2005JD006278)
34. Patra PK *et al.* 2008 TransCom model simulations of hourly atmospheric CO_2: analysis of synoptic-scale variations for the period 2002–2003. *Global Biogeochem. Cycles* **22**, GB4013. (doi:10.1029/2007GB003081)
35. Bakwin PS, Tans PP, Hurst DF, Zhao C. 1998 Measurements of carbon dioxide on very tall towers: results of the NOAA/CMDL program. *Tellus* **50B**, 401–415. (doi:10.3402/tellusb.v50i5.16216)
36. Buras A, Rammig A, Zang CS. 2020 Quantifying impacts of the drought 2018 on European ecosystems in comparison to 2003. *Biogeosciences* **17**, 1655–1672. (doi:10.5194/bg-17-1655-2020)
37. Copernicus. 2019 *European state of the climate 2018*. Reading, UK: ECMRWF.
38. Vogel MM, Zscheischler J, Wartenburger R, Dee D, Seneviratne SI. 2019 Concurrent 2018 hot extremes across Northern Hemisphere due to human-induced climate change. *Earth's Future* **7**, 692–703. (doi:10.1029/2019ef001189)
39. Reinermann S, Gessner U, Asam S, Kuenzer C, Dech S. 2019 The effect of droughts on vegetation condition in Germany: an analysis based on two decades of satellite earth observation time series and crop yield statistics. *Remote Sensing* **11**, 1783. (doi:10.3390/rs11151783)
40. Peters GP, Andrew RM, Canadell JG, Friedlingstein P, Jackson RB, Korsbakken JI, Quéré CL, Peregon A. 2019 Carbon dioxide emissions continue to grow amidst slowly emerging climate policies. *Nat. Clim. Change* **10**, 3–6. (doi:10.1038/s41558-019-0659-6)
41. Friedlingstein P *et al.* 2019 Global carbon budget 2019. *Earth Syst. Sci. Data* **11**, 1783–1838. (doi:10.5194/essd-11-1783-2019)
42. Yiou P, Nogaj M. 2004 Extreme climatic events and weather regimes over the North Atlantic: when and where? *Geophys. Res. Lett.* **31**, L07202. (doi:10.1029/2003gl019119)
43. Hertig E, Jacobeit J. 2014 Variability of weather regimes in the North Atlantic-European area: past and future. *Atmos. Sci. Let.* **15**, 314–320. (doi:10.1002/asl2.505)
44. Alvarez-Castro MC, Faranda D, Yiou P. 2018 Atmospheric dynamics leading to west European summer hot temperatures since 1851. *Complexity* **2018**, 10. (doi:10.1155/2018/2494509)
45. van der Wiel K, Bloomfield HC, Lee RW, Stoop LP, Blackport R, Screen JA, Selten FM. 2019 The influence of weather regimes on European renewable energy production and demand. *Environ. Res. Lett.* **14**, 094010. (doi:10.1088/1748-9326/ab38d3)
46. Kivi R, Heikkine P. 2016 Fourier transform spectrometer measurements of column CO_2 at Sodankylä, Finland. *Geosci. Instrum. Method. Data Syst.* **5**, 271–279. (doi:10.5194/gi-5-271-2016)
47. Sha MK *et al.* 2019 Intercomparison of low and high resolution infrared spectrometers for ground-based solar remote sensing measurements of total column concentrations of CO_2, CH_4 and CO. *Atmos. Meas. Tech. Discuss.* **2019**, 1–67. (doi:10.5194/amt-2019-371)
48. Ciais P *et al.* 2005 Europe-wide reduction in primary productivity caused by the heat and drought in 2003. *Nature* **437**, 529–533. (doi:10.1038/nature03972)
49. Lian X *et al.* 2020 Summer soil drying exacerbated by earlier spring greening of northern vegetation. *Sci. Adv.* **6**, eaax0255. (doi:10.1126/sciadv.aax0255)
50. Hakkarainen J, Ialongo I, Maksyutov S, Crisp D. 2019 Analysis of four years of global XCO_2 anomalies as seen by orbiting carbon observatory-2. *Remote Sensing* **11**, 850. (doi:10.3390/rs11070850)
51. Connor B *et al.* 2016 Quantification of uncertainties in OCO-2 measurements of XCO_2: simulations and linear error analysis. *Atmos. Meas. Tech.* **9**, 5227–5238. (doi:10.5194/amt-9-5227-2016)